

Multiacrylated Cyclodextrin: A Bio-Derived Photocurable Macromer for VAT 3D Printing

*Original*

Multiacrylated Cyclodextrin: A Bio-Derived Photocurable Macromer for VAT 3D Printing / Cosola, A., Conti, R., Grutzmacher, H., Sangermano, M., Roppolo, I., Pirri, C.F., Chiappone, A.. - In: MACROMOLECULAR MATERIALS AND ENGINEERING. - ISSN 1438-7492. - ELETTRONICO. - (2020), pp. 2000350-2000355. [10.1002/mame.202000350]

*Availability:*

This version is available at: 11583/2846021 since: 2020-09-18T09:13:16Z

*Publisher:*

Wiley-VCH Verlag

*Published*

DOI:10.1002/mame.202000350

*Terms of use:*

This article is made available under terms and conditions as specified in the corresponding bibliographic description in the repository

*Publisher copyright*

GENERICO -- per es. Nature : semplice rinvio dal preprint/submitted, o postprint/AAM [ex default]

(Article begins on next page)

**Multi-acrylated cyclodextrin: a bio-derived photocurable macromer for VAT 3D printing**

*Andrea Cosola, Riccardo Conti, Hansjörg Grützmacher, Marco Sangermano, Ignazio Roppolo, Candido Fabrizio Pirri and Annalisa Chiappone\**

A. Cosola, Prof. M. Sangermano, Dr. I. Roppolo, Prof. C. F. Pirri, Dr. A. Chiappone  
Department of Applied Science and Technology and PolitoBioMed Lab  
Politecnico di Torino  
Torino 10129, Italy  
E-mail: annalisa.chiappone@polito.it

R. Conti, Prof. H. Grützmacher  
Department of Chemistry and Applied Biosciences  
ETH Zürich  
Zürich 8093, Switzerland

Keywords: cyclodextrins, bio-derived macromer, UV-curing, vat 3D Printing

**Abstract:**

A novel cyclodextrin-derived multi-acrylated macromer (Ac- $\gamma$ -CD) was successfully prepared and tested for the generation of highly crosslinked materials by means of UV-curing. The high photo-reactivity of the macromer under UV-light irradiation was confirmed by means of real-time photorheology. Moreover, dynamic mechanical thermal analyses (DMTAs) proved that the properties of the thermosetting networks can be easily tailored by varying the concentration of the macromer in the precursor formulation. Finally, different Ac- $\gamma$ -CD based formulations were successfully used as innovative inks to reproduce several computer-aided design (CAD) files by digital light processing (DLP) 3D printing.

**Main Text:** 3D printing, also known as additive manufacturing (AM), is an intriguing production technology aimed at fabricating complex structures *via* a layer-by-layer building strategy, reproducing digital models suitably conceived for each specific application.<sup>[1]</sup> Polymeric 3D printing is beyond doubt the most widely known and especially those techniques exploiting light induced polymerization receive increasing interest.<sup>[2]</sup> These techniques, also known as VAT photopolymerization processes including stereolithography (SLA) and all its

kindred systems like digital light processing (DLP), two photons polymerization (2PP) and continuous liquid interface (CLIP), exploit a photo-chemical process to convert photocurable liquid resins into 3D solid shapes, merging microscale resolution and fast processing time.<sup>[3]</sup> Moreover, the high versatility in the formulation compounding is of great advantage of this approach. The accurate selection of each chemical compound allows the easy tailoring of structural and functional properties of the 3D printed parts.<sup>[4-10]</sup> 3D printing has been recognized as a revolutionary technology that can transform the conventional concept of manufacturing<sup>[11]</sup> but looking at the current scenario, a lot of challenges still need to be overcome to unlock its full potential, above all the enlargement of the printable materials palette. The development of polymers which are not based on fossil fuels has now become a stringent request.<sup>[12]</sup> The use of the available natural products and their derivatives can improve the value of 3D printing technologies, especially within the current framework of sustainable economy.<sup>[13]</sup> Having a closer look at the VAT 3D printing technologies, few efforts have been made in this direction up to now. Over the last years, some natural products have been (meth)acrylated or acrylated to become printable by means of SLA or DLP and most of them are specifically conceived for the preparation of hydrogels.<sup>[14-25]</sup>

Among bio-derived molecules, cyclodextrins (CDs) are interesting candidates. Cyclodextrins are macro-cyclic oligosaccharides obtained *via* the degradation of starch catalyzed by the glycosyl transferase (CGT-ase) enzyme.<sup>[26,27]</sup> They consist of several glucopyranose units arranged together to give a toroidal shape to the macro-cycle, with amphiphilic behavior. According to the number of glucose subunits, they can be classified as  $\alpha$ -CD,  $\beta$ -CD and  $\gamma$ -CD, consisting of six, seven, or eight units, respectively.<sup>[28]</sup> These molecules are particularly appealing both for their ability to form inclusion complexes with hydrophobic guests which have a suitable molecular size<sup>[29]</sup> and for their high versatility, indeed, they can be used as platform for several chemical modifications by means of hydroxyl groups substitution.<sup>[30]</sup>

In this paper we propose a highly substituted  $\gamma$ -cyclodextrin as novel photocurable multifunctional macromer for the generation of highly crosslinked materials *via* VAT 3D printing. The large availability of functionalizable sites offered by  $\gamma$ -CD allows to get a macromer bearing several reactive groups that can assure high reactivity. Therefore, a bio-derived multi-acrylated  $\gamma$ -cyclodextrin (Ac- $\gamma$ -CD) was first successfully synthesized *via* a simple procedure and then tested both as neat building block and as crosslinker for UV curing and DLP 3D printing. Once having fully investigated the photocurable formulations by means of real-time photoreology, as well as the influence of the macromer on the mechanical properties of the cured networks, 3D shaped objects were successfully printed with high resolution. Among the available natural cyclodextrins, i.e.  $\alpha$ -CD,  $\beta$ -CD and  $\gamma$ -CD, the choice fell on the latter due to the higher availability of functionalizable sites.  $\gamma$ -CD contains 24 hydroxyl groups which in principle would allow *via* a suitable acrylation protocol the synthesis of a multi-substituted cyclodextrin as reactive photocurable macromer. Acrylated- $\gamma$ -cyclodextrins (Ac- $\gamma$ -CD) were prepared following a synthetic route already reported in a previous work,<sup>[31]</sup> using acryloyl chloride as functionalizing agent (**Figure 1a**). The successful synthesis was confirmed by both  $^1\text{H}$  and  $^{13}\text{C}$  NMR, which show the characteristic signals of the new vinyl protons ( $\delta^1\text{H}=5.95, 6.18$  and  $6.32$  ppm) and carbons ( $\delta^{13}\text{C}=128.39$  and  $132.06$  ppm) as well as the signals coming from the new carbonyl carbons ( $\delta^{13}\text{C}=165.57$  ppm), respectively. The acrylation was further proved by IR spectroscopy, since in the ATR-FTIR spectrum the characteristic stretching vibration of carbonyl groups can be clearly observed at  $1727\text{ cm}^{-1}$  as well as those of vinyl groups at  $1633\text{ cm}^{-1}$ ,  $1410\text{ cm}^{-1}$  and  $808\text{ cm}^{-1}$ .<sup>[31,32]</sup> Moreover, MALDI-MS data revealed that on average approximately 90% of hydroxyl groups were acrylated, which is in accord with previous reports.<sup>[31]</sup> The synthetic route is given in the supporting information as well as all the NMR and IR data.

The multi-acrylated cyclodextrins were then tested as photocurable macromers for innovative light-sensitive inks following two different strategies as shown in Figure 1b: 1) Ac- $\gamma$ -CD as

building block of an all CD-based thermosetting polymer and 2) Ac- $\gamma$ -CD as crosslinker in combination with a mono-functional methacrylated polyethylene glycol monomer (PEGMEM). To obtain liquid formulations, the macromer was dissolved in propylene carbonate (PPC) in the first case, whereas PEGMEM itself served as reactive diluent in the second. Formulations containing increasing amounts of Ac- $\gamma$ -CD (10, 20, 30 wt%) were prepared by dispersing the macromer either in PPC or PEGMEM (depending on the strategy followed) to which BAPO-Ph [0.5 per hundred resin (phr)] was added as photoinitiator. Methyl-red (MR, 0.05 phr) was added as dye in order to assure a good print resolution by avoiding light diffusion phenomena. Prior to 3D printing, the reactivity of the multifunctional bio-derived macromer was investigated by means of real-time photo-rheology, which evaluates any variation in the rheological properties of the photocurable formulation during UV-light exposure, under constant oscillation frequency.

The plots relative to the first set of formulations (strategy 1, Ac- $\gamma$ -CD as building block) are reported in **Figure 2a**. The curves show that in all cases a CD-based thermosetting network can be easily obtained after a short irradiation time (onset of polymerization  $<2$  s) at any Ac- $\gamma$ -CD concentration (denoted as Ac $\gamma$ CD-X where X indicates the concentration as 10, 20, 30 wt%). This means that the radicals generated upon the photolysis of the photoinitiator rapidly react with the double bonds of the multi-acrylated macromer leading to the generation of a highly crosslinked network in few seconds. Also, the results show that the storage modulus ( $G'$ ) of the cured polymer gradually increases (up to 2.76 MPa for Ac $\gamma$ CD-30 wt%) by increasing the concentration of Ac- $\gamma$ -CD in the formulation. Subsequently the second set of formulations was investigated (strategy 2, Ac- $\gamma$ -CD as crosslinker of monofunctional PEGMEM, denoted as PEG-Ac $\gamma$ CD-X with X = 10, 20, 30 wt%). It is evident that increasing the amount of Ac- $\gamma$ -CD leads to the generation of thermosetting networks which are ever stiffer (Figure 2b). In fact, the  $G'$  values at the plateau level are ever-increasing (up to 11.6 MPa for PEG-Ac $\gamma$ CD-30). Furthermore, increasing the amount of Ac- $\gamma$ -CD, the photopolymerization starts earlier (onset

of polymerization from 5 s for PEG-Ac $\gamma$ CD-10 to <1 s for PEG-Ac $\gamma$ CD-30) and proceeds ever faster (from 7 kPa/s in the case of PEG-Ac $\gamma$ CD-10, to 160 kPa/s for PEG-Ac $\gamma$ CD-30), as expected when multifunctional monomers are added in a photocurable formulation due to their high reactivity and the so called “auto-acceleration” phenomenon.<sup>[33]</sup> The use of multifunctional monomers leads to the generation of highly crosslinked thermosetting networks wherein the diffusion of the radicals is strongly limited. Accordingly, while radicals’ termination mechanisms are reduced due to limited diffusion, their concentration increases leading to higher rate of photopolymerization.<sup>[33,34]</sup> Therefore, thermosetting networks are obtained at a rapidly increasing rate by increasing the content of the multi-acrylated macromer in the formulation. Note that Ac- $\gamma$ -CD itself acts as both crosslinking agent, since no crosslinking occurs by irradiating PEGMEM itself (green curve, Figure 2b), and as source of highly reactive radicals for photopolymerization. Overall, the behavior of these two sets of formulations under UV-irradiation containing a highly reactive macromer as crosslinker and polymerizable building block, suggests the use of the formulations described above for VAT 3D printing.

The thermo-mechanical properties of the cured samples were then evaluated by means of dynamic mechanical thermal analyses (DMTAs). Unfortunately, the samples prepared from the first set of formulations (Ac- $\gamma$ -CD as building block of an all CD-based network) were not suitable for these tests due to the high brittleness of the massive specimens. The DMTA curves obtained from the measurement of the PEG-Ac $\gamma$ CD-X cured samples, where X is the amount of Ac- $\gamma$ -CD in the precursor formulation, are depicted in Figure 2. All calculated parameters are summarized in **Table 1**. Figure 2c shows that all storage moduli undergo a change in the so-called glass transition region. This variation becomes lower as the amount of the multifunctional crosslinker Ac- $\gamma$ -CD in the precursor formulation is increased. In other words, the modulus at the plateau in the rubbery region, known as rubbery modulus, increased with increasing amount of Ac- $\gamma$ -CD, suggesting more rigid networks. This rubbery modulus has been related to the crosslinking density ( $\nu_e$ ) of the thermosetting network by several theories,<sup>[33,35]</sup>

suggesting that higher moduli indicate higher crosslinking density. According to the values reported in Table 1,  $v_e$  increases as expected by increasing the amount of Ac- $\gamma$ -CD (from 0.0025 mmol/mm<sup>3</sup> up to 0.0768 mmol/mm<sup>3</sup>). Furthermore, the shift of the  $\tan\delta$  curves towards higher temperatures (Figure 2d) shows, that the glass transition temperature ( $T_g$ ) of the polymer network increases with increasing amount of crosslinker.

The increase of the crosslinking density induced by higher Ac- $\gamma$ -CD content implies a decrease in the mobility of the PEGMEM chain, which is reflected by higher  $T_g$ . Moreover, the  $\tan\delta$  curves become broader and are flattened as the crosslinker content is increased. Broader curves imply a more heterogeneous network with a broader distribution of chain relaxation or mobilities within the polymer matrix which means the  $T_g$  is spread over a wide region.<sup>[36-38]</sup> However, here the  $T_g$  is reported as the temperature corresponding to the  $\tan\delta$  peak, as recommended by traditional conventions. This  $\tan\delta$  broadening proves further the generation of highly crosslinked networks using Ac- $\gamma$ -CD as multi-acrylated macromer and this complex phenomenon is typical for heterogeneous thermosetting networks generated by photopolymerization of multifunctional monomers.<sup>[33,39]</sup> The structural heterogeneity can be ascribed to the generation of highly crosslinked regions with reduced mobility, named microgels, and to less crosslinked microregions.<sup>[40,41]</sup> Therefore, looking at the curves, the inhomogeneity of the network increases by increasing the content of the multi-functional macromer. The mechanical properties of the cured samples were also investigated by means of amplitude sweep measurements (AS). The results confirm further the increase of the rigidity with higher amount of multifunctional macromer (**Figure S1**) since the recorded storage modulus increases by increasing the amount of Ac- $\gamma$ -CD and, at the same time, the cured samples can endure a lower strain amplitude before breaking. It is therefore evident that the accurate compounding of the formulations allows to tailor the thermo-mechanical properties of the resulting thermosetting networks.

Finally, different Ac $\gamma$ CD-X and PEG-Ac $\gamma$ CD-X formulations were tested as innovative inks for DLP 3D printing. Those containing either 20 wt% or 30 wt% of Ac- $\gamma$ -CD were chosen as best candidates because of the combination of favorable properties, namely (i) short induction time during photopolymerization, (ii) fast curing rate, and (iii) high mechanical stability, as honeycomb structures to more complex hollow-lattice parts, were reproduced using a commercial DLP printer. The printing parameters were carefully investigated for each formulation. In particular, the layer thickness was fixed to 50  $\mu\text{m}$  and the UV-light intensity to 30.66  $\text{mW cm}^{-2}$ , while the exposure time was ranged from 1.5 to 2.5 s/layer according to the preliminary photorheology tests. Highly complex structures with defined details in the order of 200  $\mu\text{m}$  could be successfully printed using the precursor formulations mentioned above (**Figure 3** and **Figure S2**). Further, the printed parts show high geometrical fidelity to the CAD models since very low dimensional variations were detected, as confirmed by the comparison between the dimension of the smallest features of the 2D section of CAD model b and the corresponding optical microscopy images (Figure 3c).

However, those structures fabricated from all-CD based inks result much more brittle than the ones printed using the set of formulation wherein Ac- $\gamma$ -CD acts as crosslinker of monofunctional PEGMEM. This can be ascribed to the different nature of the thermosetting network generated upon irradiation. In fact, whilst both systems are very highly crosslinked, the presence of PEGMEM limits the brittleness since the monofunctional monomer acts as plasticizer improving the flexibility of the printed structure.

In conclusion, the current work describes the use of multi-acrylated cyclodextrins (Ac- $\gamma$ -CDs) as novel bio-derived macromers for UV-curing and VAT polymerization 3D printing. Real-time photorheology measurements confirmed the high reactivity of Ac- $\gamma$ -CD upon UV-light irradiation, suggesting its potential use as both neat building block and as crosslinker for the generation of highly crosslinked thermosetting networks. The thermo-mechanical analysis revealed the high versatility of the system PEG-Ac $\gamma$ CD-X (X = 10, 20, 30 wt%). An accurate

compounding of the formulations allows to easily tailor the mechanical properties of the cured samples, exploiting the high crosslinking efficiency of Ac- $\gamma$ -CD and the plasticizing effect induced by PEGMEM. Finally, the highly defined 3D printed structures confirmed the potential use of different photocurable formulations containing Ac- $\gamma$ -CD as innovative inks for VAT polymerization techniques. Exploiting the intriguing characteristics of CDs, future studies will now focus on 4D bio-based functional printing which is in reach.

### Supporting Information

Supporting Information is available from the Wiley Online Library or from the author.

### Acknowledgements

This work was performed with the financial support of Compagnia di San Paolo and the Swiss national Science Foundation via grant SNF 2-77020-17.

Received: ((will be filled in by the editorial staff))

Revised: ((will be filled in by the editorial staff))

Published online: ((will be filled in by the editorial staff))

### References

- [1] T. D. Ngo, A. Kashani, G. Imbalzano, K. T. Q. Nguyen and D. Hui, *Compos. Part B Eng.* **2018**, *143*, 172.
- [2] X. Wang, M. Jiang, Z. Zhou, J. Gou and D. Hui, *Compos. Part B Eng.* **2017**, *110*, 442.
- [3] M. Layani, X. Wang and S. Magdassi, *Adv. Mater.* **2018**, *30*, 1706344.
- [4] J. Stampfl, S. Baudis, C. Heller, R. Liska, A. Neumeister, R. Kling, A. Ostendorf and M. Spitzbart, *IOP Publ. J. MICROMECHANICS MICROENGINEERING J. Micromech. Microeng* **2008**, *18*, 9.
- [5] V. C. F. Li, X. Kuang, A. Mulyadi, C. M. Hamel, Y. Deng and H. J. Qi, *Cellulose* **2019**, *26*, 3973.
- [6] A. Chiappone, E. Fantino, I. Roppolo, M. Lorusso, D. Manfredi, P. Fino, C. F. Pirri and F. Calignano, *ACS Appl. Mater. Interfaces* **2016**, *8*, 5627.

- [7] S. Lantean, G. Barrera, C. F. Pirri, P. Tiberto, M. Sangermano, I. Roppolo and G. Rizza, *Adv. Mater. Technol.* **2019**, *4*, 1900505.
- [8] M. Gillono, I. Roppolo, F. Frascella, L. Scaltrito, C. F. Pirri and A. Chiappone, *Appl. Mater. Today* **2020**, *18*, 100470.
- [9] Q. Ge, A. H. Sakhaei, H. Lee, C. K. Dunn, N. X. Fang and M. L. Dunn, *Sci. Rep.* **2016**, *6*, 1.
- [10] A. Zhakeyev, L. Zhang and J. Xuan, *3D and 4D Printing of Polymer Nanocomposite Materials: Processes, Applications, and Challenges*, Elsevier, **2019**, pp. 387–425.
- [11] S. C. Ligon, R. Liska, J. Stampfl, M. Gurr and R. Mülhaupt, *Chem. Rev.* **2017**, *117*, 10212.
- [12] J. Liu, L. Sun, W. Xu, Q. Wang, S. Yu and J. Sun, *Carbohydr. Polym.*, **2019**, *207*, 297.
- [13] J. Huang, S. Fu and L. Gan, *Lignin chemistry and applications*, Elsevier, **2019**.
- [14] R. Ding, Y. Du, R. B. Goncalves, L. F. Francis and T. M. Reineke, *Polym. Chem.* **2019**, *10*, 1067.
- [15] S. Miao, W. Zhu, N. J. Castro, M. Nowicki, X. Zhou, H. Cui, J. P. Fisher and L. G. Zhang, *Sci. Rep.* **2016**, *6*, 1.
- [16] V. S. D. Voet, T. Strating, G. H. M. Schnelting, P. Dijkstra, M. Tietema, J. Xu, A. J. J. Woortman, K. Loos, J. Jager and R. Folkersma, *ACS Omega* **2018**, *3*, 1403.
- [17] J. T. Sutton, K. Rajan, D. P. Harper and S. C. Chmely, *ACS Appl. Mater. Interfaces* **2018**, *10*, 36456.
- [18] A. C. Weems, K. R. Delle Chiaie, J. C. Worch, C. J. Stubbs and A. P. Dove, *Polym. Chem.* **2019**, *10*, 5959.
- [19] J. Guit, M. B. L. Tavares, J. Hul, C. Ye, K. Loos, J. Jager, R. Folkersma and V. S. D. Voet, *ACS Appl. Polym. Mater.* **2020**, *2*, 949.
- [20] A. C. Weems, K. R. Delle Chiaie, R. Yee and A. P. Dove, *Biomacromolecules* **2020**, *21*, 163.

- [21] P. Zorlutuna, J. H. Jeong, H. Kong and R. Bashir, *Adv. Funct. Mater.* **2011**, *21*, 3642.
- [22] S. Suri, L. H. Han, W. Zhang, A. Singh, S. Chen and C. E. Schmidt, *Biomed. Microdevices* **2011**, *13*, 983.
- [23] K. Na, S. Shin, H. Lee, D. Shin, J. Baek, H. Kwak, M. Park, J. Shin and J. Hyun, *J. Ind. Eng. Chem.* **2018**, *61*, 340.
- [24] S. H. Kim, Y. K. Yeon, J. M. Lee, J. R. Chao, Y. J. Lee, Y. B. Seo, M. T. Sultan, O. J. Lee, J. S. Lee, S. I. Yoon, I. S. Hong, G. Khang, S. J. Lee, J. J. Yoo and C. H. Park, *Nat. Commun.* **2018**, *9*, 1.
- [25] J. K. Placone, J. Navarro, G. W. Laslo, M. J. Lerman, A. R. Gabor, G. J. Herendeen, E. E. Falco, S. Tomblyn, L. Burnett and J. P. Fisher, *Ann. Biomed. Eng.* **2017**, *45*, 237.
- [26] A. Villiers, *Compt Rend Acad Sci* **1891**, *112*, 536.
- [27] A. Biwer, G. Antranikian and E. Heinzle, *Appl. Microbiol. Bio-technol.* **2002**, *59*, 609.
- [28] E. M. M. Del Valle, *Process Biochem.* **2004**, *39*, 1033.
- [29] S. V. Kurkov and T. Loftsson, *Int. J. Pharm.* **2013**, *453*, 167.
- [30] M. Řezanka, *Environ. Chem. Lett.* **2019**, *17*, 49.
- [31] A. Cosola, R. Conti, V. K. Rana, M. Sangermano, A. Chiappone, J. Levalois-Grützmacher and H. Grützmacher, *Chem. Commun.* **2020**, *56*, 4828.
- [32] E. S. Gil, L. Xiu and T. L. Lowe, *Biomacromolecules* **2012**, *13*, 3533.
- [33] K. S. Anseth, C. M. Wang and C. N. Bowman, *Polymer (Guildf)*. **1994**, *35*, 3243.
- [34] T. G. Fox and S. Loshaek, *J. Polym. Sci.* **1955**, *15*, 371.
- [35] J. M. Charlesworth, *Polym. Eng. Sci.* **1988**, *28*, 230.
- [36] G. P. Simon, P. E. M. Allen and D. R. G. Williams, *Polymer (Guildf)*. **1991**, *32*, 2577.
- [37] P. E. M. Allen, A. B. Clayton and D. R. G. Williams, *Eur. Polym. J.* **1994**, *30*, 427.
- [38] S. S. Edwards, *Polym. Int.* **1993**, *32*, 435.
- [39] J. Park, J. Eslick, Q. Ye, A. Misra and P. Spencer, *Dent. Mater.* **2011**, *27*, 1086.

[40] A. R. Kannurpatti, J. W. Anseth and C. N. Bowman, *Polymer (Guildf)*. **1998**, *39*, 2507.

[41] W. D. Cook, *Thermal aspects of the kinetics of dimethacrylate photopolymerization*, Elsevier, **1992**.

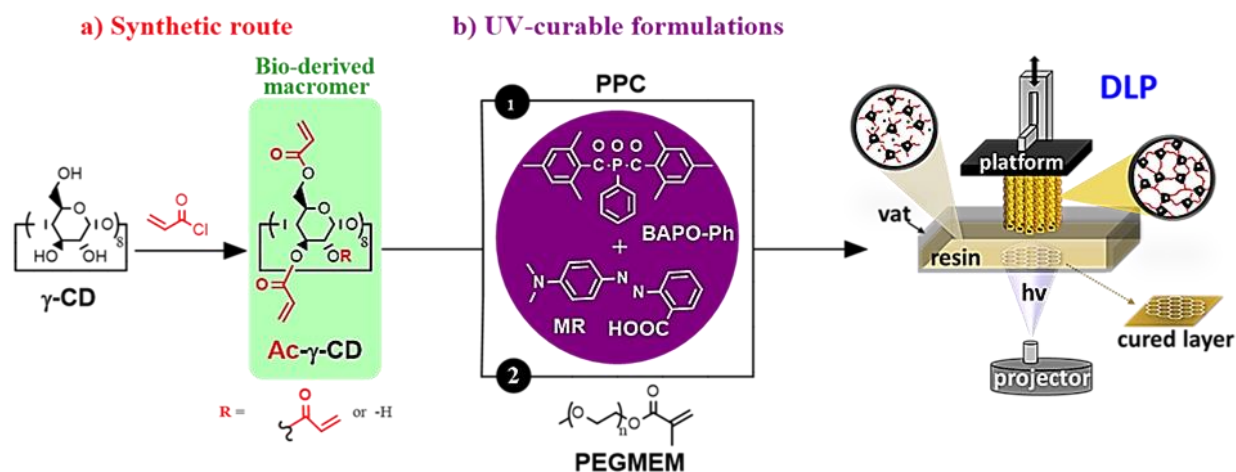


**Figure 1.** Schematic representation of a) synthesis of the bio-derived macromer Ac- $\gamma$ -CD and b) two different strategies applied to prepare a photocurable formulation suitable for Digital Light Processing (DLP) 3D-Printing.

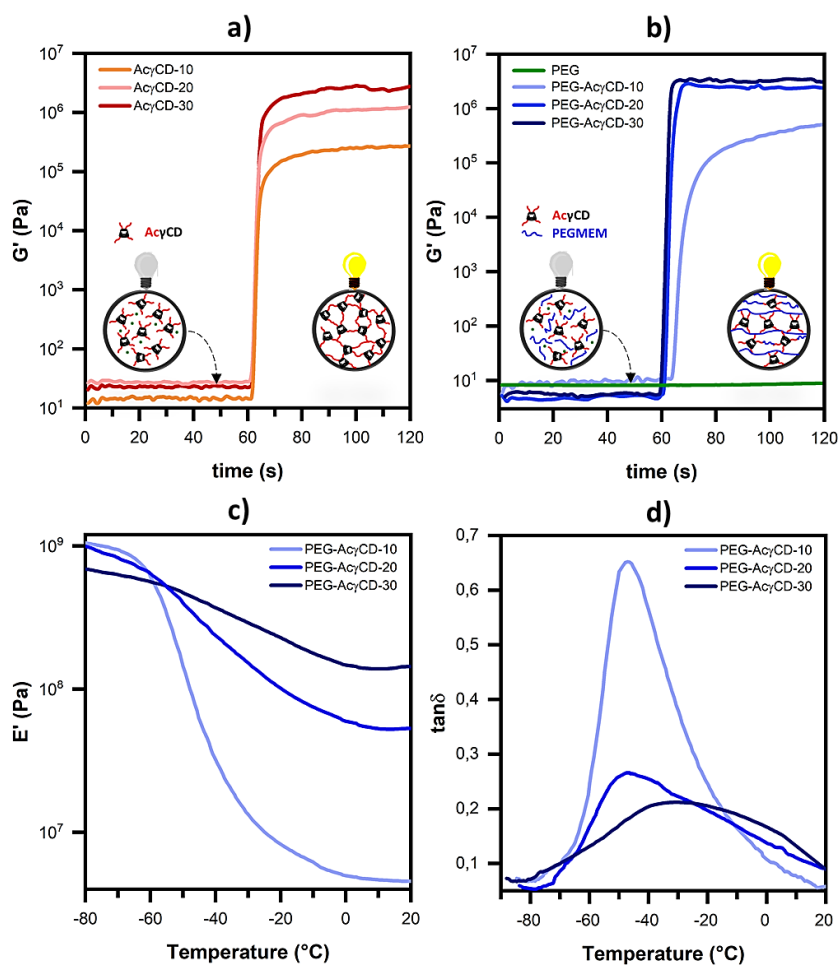


**Figure 2.** Photorheology characterization and corresponding photopolymerization mechanisms of the two different set of formulations using Ac- $\gamma$ -CD as a) building block or as b) crosslinker of monofunctional PEGMEM, and thermo-mechanical characterization of the cured sample prepared from formulations PEG-Ac $\gamma$ CD-X: c)  $E'$  plots and d)  $\tan\delta$  curves.

**Table 1.** Thermo-mechanical properties of the cured samples prepared from formulations PEG-Ac $\gamma$ CD-X.

Sample	$E'_{r.t.}$ (Pa)	$\tan\delta$	$T_g$ ( $^{\circ}$ C)	$v_e$ (mmol mm $^{-3}$ )
PEG-Ac $\gamma$ CD-10	$4.5 \times 10^6$	0.66	-48	0.0025
PEG-Ac $\gamma$ CD-20	$5.1 \times 10^7$	0.26	-45	0.0280
PEG-Ac $\gamma$ CD-30	$1.4 \times 10^8$	0.21	-30	0.0768

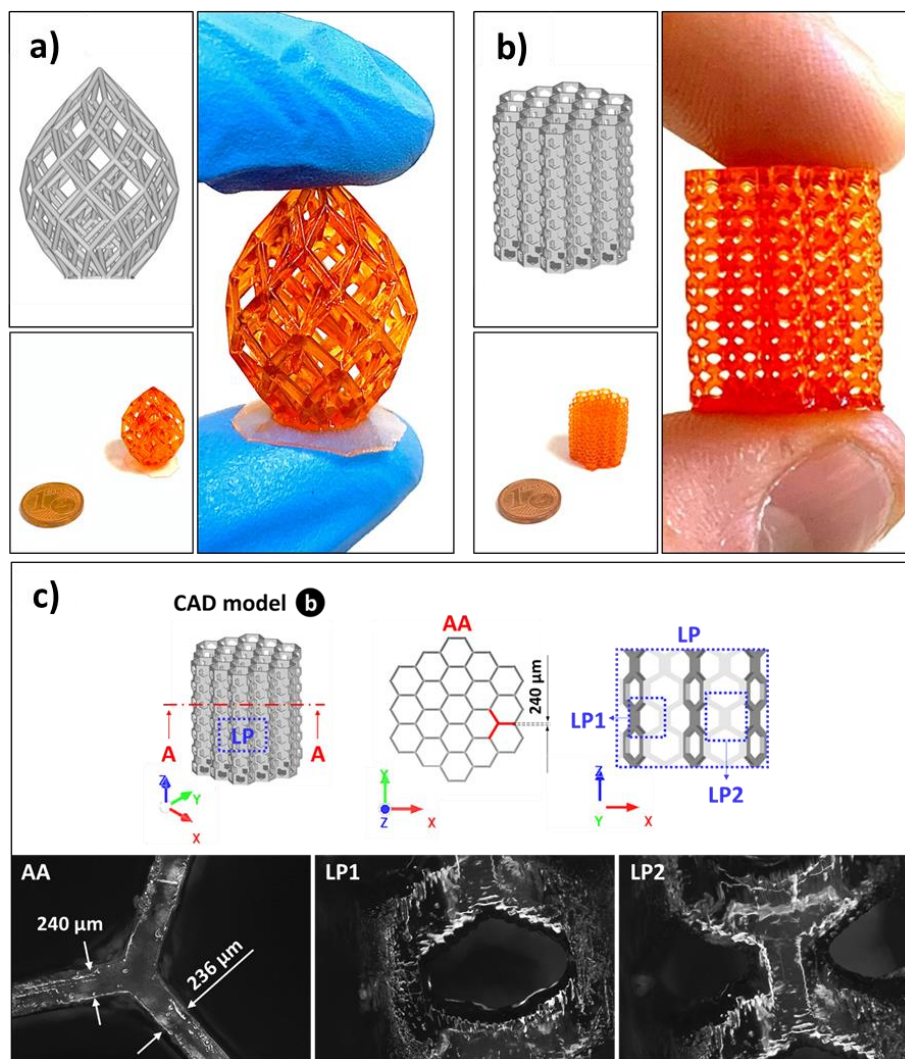


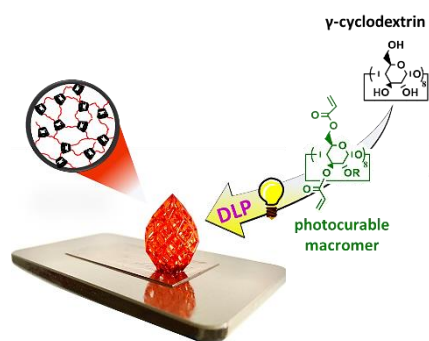
**Figure 3.** Photographs of different 3D printed structures (a and b) from PEG-Ac $\gamma$ CD-20 and their corresponding digital CAD design and (c) light microscope images corresponding to section AA and lateral views LP1/LP2 of the 3D printed structure of component (b).

### Multi-acrylated cyclodextrin: a bio-derived photocurable macromer for VAT 3D printing

*Andrea Cosola, Riccardo Conti, Hansjörg Grützmaier, Marco Sangermano, Ignazio Roppolo, Candido Fabrizio Pirri and Annalisa Chiappone\**

ToC entry: In this work, a multi-acrylated cyclodextrin-derived macromer (Ac- $\gamma$ -CD) is successfully prepared and tested for the generation of highly crosslinked materials by means of digital light processing (DLP) 3D printing

ToC figure:



## Supporting Information

### **Multi-acrylated cyclodextrin: a bio-derived photocurable macromer for VAT 3D printing**

*Andrea Cosola, Riccardo Conti, Hansjörg Grützmacher, Marco Sangermano, Ignazio Roppolo, Candido Fabrizio Pirri and Annalisa Chiappone\**

#### **Materials**

$\gamma$ -Cyclodextrin ( $M_n = 1297.14$  g/mol) was obtained from ABCR. Acryloyl chloride, n-methyl pyrrolidone (NMP), propylene carbonate (PPC), poly(ethylene glycol) methyl ether methacrylate (PEGMEM,  $M_n = 500$  g/mol), phenylbis(2,4,6-trimethylbenzoyl)phosphine oxide (BAPO-Ph) and methyl red (MR) were purchased from Sigma Aldrich and used without further purification.

#### **Solution NMR spectroscopy**

$^1\text{H}$  NMR and  $^{13}\text{C}$  NMR spectra were recorded on Bruker 300 spectrometer operating at 300.13 MHz and 75.47 MHz, respectively. Chemical shifts ( $\delta$ ) were measured according to IUPAC and are given in parts per million (ppm) relative to TMS and  $\text{H}_3\text{PO}_4$  for  $^1\text{H}$  NMR and  $^{13}\text{C}\{^1\text{H}\}$  NMR, respectively.

#### **IR spectroscopy**

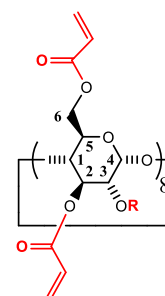
Attenuated total reflection (ATR) spectra were collected using a Tensor 27 FTIR spectrometer. 32 spectra were collected for each sample in the range of  $4000\text{--}600\text{ cm}^{-1}$  with a resolution of  $4\text{ cm}^{-1}$ .

### Maldi mass spectrometry

Mass spectrometry measurements were carried out by the MS Service of the Laboratory of Organic Chemistry at ETH Zürich. Experimental parameter: positive polarity, laser power 27.6 lp, time to flight to 0.004 sec, nebulizer gas 1.3 bar, drying gas flow rate 3.7 L/min, capillary 3000.0 V, drying gas temperature 200.0 °C.

### Synthesis of multi-acrylated $\gamma$ -Cyclodextrin (Ac- $\gamma$ -CD)

Ac- $\gamma$ -CD was prepared according to a synthetic route already reported in a previous work.<sup>[1]</sup> The numbers 1-6 given in the figure on the right refer to the relative position of H and C atoms in the glucopyranose subunits of CD. Once being dried at 90 °C under vacuum for 24 h,  $\gamma$ -Cyclodextrin ( $\gamma$ -CD, 20 g, 15.42 mmol, 1 eq.) was charged in a 500 mL Schlenk flask containing 160 mL of anhydrous n-methyl-pyrrolidone (NMP) and the reaction



**AC- $\gamma$ -CD**

mixture was left to stir under Argon atmosphere until the solution became homogeneous. Then acryloyl chloride (36.07 mL, 0.44 mol, 28.8 eq.) was added dropwise at 0 °C and the reaction mixture left to stir for 72 h at r.t. and 300 rpm. Dropping slowly the mixture into 2 L of deionized H<sub>2</sub>O yields Ac- $\gamma$ -CD as a white precipitate. After decanting the mixture for 30 min. at r.t., Ac- $\gamma$ -CD (36.6 g, 67%) was filtered and washed four times using DI-H<sub>2</sub>O. Finally, the product was dried for two days under high vacuum before characterization by means of <sup>1</sup>H NMR, <sup>13</sup>C NMR and MALDI-MS.

**<sup>1</sup>H NMR** (300.13 MHz, DMSO-*d*<sub>6</sub>,  $\delta$ ): 2.86 - 5.24 (H<sup>1</sup>, H<sup>2</sup>, H<sup>3</sup>, H<sup>4</sup>, H<sup>5</sup> and H<sup>6</sup>)<sub>gluc. subunits</sub>, 5.95 (-CH=CH<sub>2</sub>), 6.18 (CH=CH<sub>2</sub>) and 6.32 (-CH=CH<sub>2</sub>).

**<sup>13</sup>C NMR** (75.47 MHz, DMSO-*d*<sub>6</sub>,  $\delta$ ): 63.52 (C<sup>6</sup>), 69.54 (C<sup>5</sup>)<sub>gluc. subunits</sub>, 72.94 (C<sup>3</sup>)<sub>gluc. subunits</sub>, 73.11 (C<sup>2</sup>)<sub>gluc. subunits</sub>, 81.88 (C<sup>4</sup>)<sub>gluc. subunits</sub>, 102.22 (C<sup>1</sup>)<sub>gluc. subunits</sub>, 128.39 (-CH=CH<sub>2</sub>), 132.06 (CH=CH<sub>2</sub>) and 165.57 (-C=O).

**IR:** 1727  $\text{cm}^{-1}$  ( $\nu\text{C}=\text{O}$ ), 1633  $\text{cm}^{-1}$  ( $\nu\text{C}=\text{C}$ ), 1410  $\text{cm}^{-1}$  ( $\nu\text{H}-\text{C}=\text{CH}_2$ ), 1297  $\text{cm}^{-1}$  ( $\nu\text{C}-\text{O}$ )<sub>unsat.  $\alpha$ - $\beta$</sub> , 1156  $\text{cm}^{-1}$  ( $\nu\text{C}-\text{O}-\text{C}$ )<sub>gluc. subunits.</sub>, 1080  $\text{cm}^{-1}$  ( $\nu\text{C}-\text{O}$ )<sub>6,gluc. subunits.</sub>, 1024  $\text{cm}^{-1}$  ( $(\nu\text{C}-\text{C}) + (\nu\text{C}-\text{O})$ )<sub>gluc. subunits</sub> and 809 ( $\nu\text{C}-\text{H}$ ).

**MALDI-MS:**  $M_w = 2450$  g/mol (average molecular weight calculated from the normal distribution of the  $m/z$  peaks).<sup>[1,2]</sup> According to these data, almost 90% of the OH groups (21/24) were successfully substituted on average.

### Preparation of the photocurable formulations

The bio-derived multi-acrylated macromer Ac- $\gamma$ -CD was used to prepare two sets of light responsive formulations.

In the first case different amounts of Ac- $\gamma$ -CD i.e. 10, 20 and 30 wt% were dispersed in PPC. Then, 0.5 phr (per hundred resin) of BAPO-Ph as photoinitiator and 0.05 phr of MR as photosensible dye absorber were added and the mixture was stirred until it became homogeneous. This set of samples was named Ac- $\gamma$ -CD-X (X corresponding to the wt% of Ac- $\gamma$ -CD used).

In the second case different amounts of Ac- $\gamma$ -CD i.e. 10, 20 and 30 wt% were dispersed in PEGMEM, a monofunctional methacrylate monomer used as reactive diluent. Subsequently, as already reported for the preparation of the first set, 0.5 phr of BAPO-Ph and 0.05 phr of MR were added and the mixture was stirred until complete dissolution. These formulations were named PEG-Ac $\gamma$ CD-X, (X corresponding to the wt% of Ac- $\gamma$ -CD used).

### Rheology

The reactivity of the photocurable formulations was investigated by means of photorheology using an Anton PAAR Modular Compact Rheometer (Physica MCR 302, Graz, Austria) in parallel-plate mode (25 mm diameter). The photocuring kinetics of the formulations was evaluated *via* real-time measurements carried out at room temperature (r.t., 25°C), using a UV-

curing set-up inclusive of a quartz bottom plate and a UV-light source (Hamamatsu LC8 lamp equipped with a 8 mm light guide,  $30 \text{ mW cm}^{-2}$ ) underneath the bottom plate. During the measurements, the gap between the two glass plates was set to 0.2 mm and the sample was kept under a constant shear frequency (10 Hz). Light was switched on after 60 s to assure the stability of the system before the onset of photopolymerization. According to preliminary amplitude sweep measurements, all the tests were carried out in the linear viscoelastic region setting a strain amplitude of 0.8 %. The variation of the storage modulus ( $G'$ ) was recorded as a function of the irradiation time. The onset of photopolymerization (i.e. the delay time required to induce crosslinking) and the curing rate (measured as the slope of the curve in the first 20 s of irradiation) were also investigated.

Afterwards, amplitude sweep measurements (AS) were performed on the cured samples at r.t. ( $25 \text{ }^\circ\text{C}$ ) from 0.01% to 1000% and under a constant shear frequency (10 Hz), in order to determine the limit of the viscoelastic region.

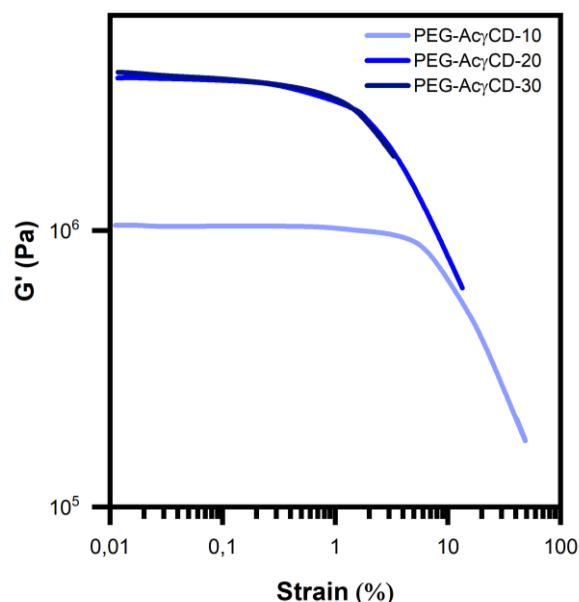


**Figure S1** Amplitude sweep measurements performed on the cured samples from formulations PEG-Ac $\gamma$ CD-X.

### **Dynamic mechanical thermal analyses (DMTA)**

Flat samples (20 mm x 10 mm x 0.5 mm) were prepared by casting into silicon molds the photocurable formulations and irradiating for 60 s under nitrogen atmosphere, using a Dymax ECE 5000-UV lamp (320-390 nm).

Dynamic mechanical thermal analysis (DMTAs) was used to investigate the thermo-mechanical properties of the cured samples. The measurements were performed with a Tritec 2000 DMA (Triton Technology Ltd, London UK). All of the experiments were carried out between -90°C and 25 °C setting a temperature ramp of 3°C/min and applying a force to the sample under a frequency of 1 Hz with a displacement of 20 µm. The variation of both the elastic modulus ( $E'$ ) and the damping factor ( $\tan\delta$ , calculated as the ratio between the loss and storage modulus) were measured as a function of the temperature. The glass transition temperature ( $T_g$ ) was measured as the temperature corresponding to the maximum of the  $\tan\delta$  curve.

### **Crosslinking density**

The crosslinking density ( $\nu_e$ ) of the cured samples was calculated as number of moles of crosslinking point per unit of volume, according to the statistical theory of rubber elasticity using the equation:  $E' = \nu_e RT$ .<sup>3</sup> Where  $E'$  is elastic modulus above  $T_g$ ,  $T$  is the temperature and  $R$  is the universal gas constant.

### **3D Printing**

Different formulations were then 3D printed using a UV-MAX X27 DLP printer (ASIGA) with a building volume of 119 mm x 67 mm x 75 mm, a nominal XY pixel resolution of 27 µm and a light-emitting diode light source (385 nm, 32 mW cm<sup>-2</sup>). Several CAD models were converted in STL file formats and 3D printed. At last, the printed objects were post-cured under UV-light (4 min, 12 mW cm<sup>-2</sup>) using a medium-pressure mercury lamp provided by Robot Factory.

Optical images of the samples were collected with a Leica DM2500 microscope, in order to investigate the final resolution of the printed structures and their fidelity to the corresponding CAD digital models.

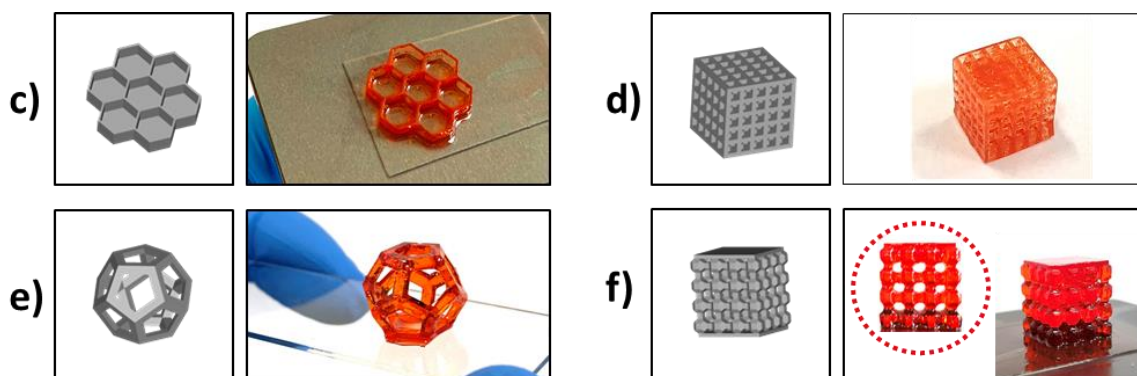


**Figure S2** Photographs of different 3D printed structures (c-d from Ac $\gamma$ CD-30; e-f from PEG-Ac $\gamma$ CD-20) and their corresponding digital CAD design.

## References

- [1] A. Cosola, R. Conti, V. K. Rana, M. Sangermano, A. Chiappone, J. Levalois-Grützmacher and H. Grützmacher, *Chem. Commun.* **2020**, 56, 4828.
- [2] E. S. Gil, L. Xiu and T. L. Lowe, *Biomacromolecules* **2012**, 13, 3533.
- [3] A. Chiappone, S. Jeremias, R. Bongiovanni, M. Schönhoff, *Journal of Polymer Science Part B: Polymer Physics* **2013**, 51, 1571.